Self-energy corrections to the *ab initio* band structure: Chromium

N. I. Kulikov,* M. Alouani, and M. A. Khan
Laboratoire de Magnétisme et de Structure Electronique des Solides, Université Louis Pasteur, 4, rue Blaise Pascal 67070 Strasbourg Cedex, France

M. V. Magnitskaya
L. F. Veregschagin Institute of High Pressure Physics, Academy of Science of USSR, 142092 Troitsk, Moscow Region, USSR
(Received 17 December 1986)

We describe the effect of many-particle corrections to improve the electronic energy spectrum calculated in the framework of the density functional formalism (DFF). We show that it is possible to consider an n-particle diagram like a correction to the DFF results for electronic structure, if we take into account the electron-electron interaction with nonzero transmitted momentum q or energy ε. A model is proposed for calculating the leading term of the self-energy expansion as a power series in interactions, i.e., the second-order term under the conditions $q=0$ and $\varepsilon\neq 0$. This model is illustrated by calculating the electronic band structure and optical properties of antiferromagnetic chromium. The self-energy correction leads to a better agreement between the theoretical calculations and experimental measurements of electronic properties.

I. INTRODUCTION

At the present time, it is universally accepted that the one-particle band structures obtained by the numerical *ab initio* calculations give a good description of the measured electronic properties. However, it should be noted that the theorem by Hoenberg and Kohn[1] was proved only for the properties of the ground state, for example, cohesive energy, bulk modulus, spontaneous magnetic moments, etc. The theorem declared that these properties can be determined by a unique functional of the electronic density which is calculated by using the one-particle Schrödinger equation with a local effective potential.[2] It should be emphasized that the same one-particle spectrum, which has given an exact description of the ground-state properties does not necessarily give a satisfactory description of the electronic properties.

The x-ray and ultraviolet photoemission spectra (XPS and UPS) where valence electrons are excited by photons with high frequencies, optical properties, and even the resonance frequencies of the de Haas–van Alphen effect may serve as examples of the electronic properties measured by excitations of the ground state.

Obviously in the framework of the density functional formalism (DFF) the band structure is determined only through correspondence between the total energies of the interacting electron system and the fictitious one-particle system.[2,3] Formally the band structure of the one-particle system cannot have any common feature with dispersed quasiparticle states. The practice of band-structure calculations shows that it is not so important and qualitatively the local-density approximation (LDA) of DFF allows us to calculate band structures which predict a large part of experimental results concerning electronic properties.[3,4]

However, it should be noted that the deviation between experiments and results of band structure calculations increase with the rise of the excitation energy. Moreover, a number of recent calculations have revealed significant deviations of LDA band structures from experimental data. For example, calculated widths of the valence band of transition metals are 1–2 eV narrower than measured widths in XPS and UPS experiments. In the case of Ni we are confronted with a set of problems: the presence of a satellite in the XPS spectrum, the narrowing of the d bandwidth, the reduction of the exchange splitting, etc. The calculated values of the dielectric gap for insulators and semiconductors are less than the experimental value by a factor of 2. There have been great efforts during the last few years to improve the calculated optical spectrum of semiconductors.[5–8] The quasiparticle energies in semiconductors and insulators are described in terms of the electron self-energy operator. The self-energy operator is evaluated in the so-called GW approximation, where one uses the dynamically screened Coulomb interaction (W) and the dressed Green function (G). This theoretical development has given excellent results for the forbidden gaps in Si, Ge, and LiCl.[7,8]

The optical measurements in the metals have a good agreement with band-structure calculations within the infrared range of the excitation energy but an increase of photon energies leads to a rise in deviations between calculations and experiments. The possible reason for the deviation is the local approximation to the exchange-correlation part of the effective crystal potential. In order to avoid misunderstanding it should be noted that two kinds of nonlocality exist in this problem. On one hand the crystal potential can be calculated in the LDA approach. It means that the exchange-correlation potential can be written[3,9] in the following form:

$$V_{\rm xc}(r_2)=\int d^3r_1\, V(r_{12})Q_{\rm xc}(r_1,r_2)\ , \tag{1}$$

where $V(r_{12})=1/|r_1-r_2|$ and the expression

$$Q_{xc}(r_1,r_2)=n(r_1)[g(r_1,r_2)-1] \quad (2)$$

describes a density of an exchange-correlation hole created by interactions in the electron system. The LDA means that we used the pair correlation function $g(r_1,r_2)$ for the homogeneous electron liquid at the local density $n(r_1)$.

In this work we will discuss primarily another type of nonlocality which concerns the nonlocal nature of the effective potential determined for the quasiparticles spectrum. In what follows we shall attempt to show that the possibility to introduce many-particle corrections to the band structure calculated in the framework of DFF theory really exists.

Mc Alister *et al.*[10] compared the experimental XPS and UPS data with the results of a great number of band-structure calculations of 3d transition metals. This comparison showed a reasonable agreement except in the case of Ni, where experimental bands are 1.5–2 eV narrower than those given by available calculations. But for the most part these earlier calculations were performed by using non-self-consistent crystal potentials with Slater exchange. Later, more correct self-consistent *ab initio* band-structure calculations with the LDA Hedin-Lundqvist[11] exchange-correlation potential were made. Such types of calculations show a good agreement with experiments in the case of Cu (Ref. 12) (although the calculated bands are wider), but the agreement between the theory and the experiment becomes worse for other transition metals. For example, cobalt and chromium have calculated bands 10–20% wider than experimental bands.[13,14] The same situation occurs in the case of Fe and Ni.[15]

It is also very useful to compare the calculated joint density of states with the measurements of optical conductivity. Such comparisons have been performed in recent years in many papers.[13,16,17] It is noticed that the predicted positions deviate more from the experimental optical transitions when the energy of excitation increases. Very good agreement was obtained in the case of Cu,[13,17] where the *d* band is filled, but the same quantitative agreement in the case of Cr (Refs. 16 and 18) and Ni (Ref. 15) is not obtained.

Now, from this short review, the following points have been established.

(i) A systematic deviation between self-consistent LDA calculations and experimental values occurs. Moreover, the deviations become large when excitation energy increases. However in some cases, for example the case of copper, the deviation is relatively small.

(ii) Some effective potentials[19,20] give better agreement with experiments than the existing self-consistent *ab initio* LDA. It is useful to note the success of the "second-principle" approach[21,22] where a good description of electronic properties is obtained by using the fitting scheme in the framework of the band-structure calculations.

The remainder of this paper is organized as follows. In Sec. II we discuss the possibility of using the perturbation theory for the corrections to the band structure within the DFF approach. The method of band-structure calculation is presented and band-structure results for Cr are given in Sec. III. The model for the calculation of many-particle corrections is discussed. Finally, we discuss the influence of many-particle corrections in Sec. IV where the optical properties obtained from calculations are compared with experiments.

II. PERTURBATION THEORY AND DFF APPROACH

The Green functions used in many-body theory are useful generalizations of the ordering Green functions. The full Green function is determined by the Dyson equation (see, for example, Ref. 23):

$$G(r_1,r_2,\varepsilon)=G_0(r_1,r_2,\varepsilon)+\int G_0(r_1,r_3,\varepsilon)\Sigma(r_3,r_4,\varepsilon) \times G(r_4,r_2)dr_3\,dr_4 , \quad (3)$$

where $G_0(r_1,r_2,\varepsilon)$ is the Green function of the free-electron system which is given by

$$(-\nabla^2+\varepsilon)G_0(r,r',\varepsilon)=\delta(r-r') , \quad (4)$$

and $\Sigma(r,r',\varepsilon)$ is the self-energy operator. Multiplying Eq. (3) by $(-\nabla^2+\varepsilon)$ we obtain

$$(-\nabla^2+\varepsilon)G(r_1,r_2,\varepsilon) - \int \Sigma(r_1,r_3,\varepsilon)G(r_3,r_2,\varepsilon)dr_3=\delta(r_1-r_2) . \quad (5)$$

The inhomogeneous equation (5) is connected with the Schrödinger-type equation, e.g.,

$$(-\nabla^2+E_k)\phi_k(r_1)-\int \Sigma(r_1,r_2,E_k)\phi_k(r_2)dr_2=0 \quad (6)$$

which determined the quasiparticle spectrum E_k.

In this integro-differential equation (6) the self-energy Σ can be considered as a nonlocal effective potential for an electron-electron interaction and it can be written as

$$\Sigma(r,r',\varepsilon)=\delta(r-r')\delta(\varepsilon)v_H(r)+M(r,r',\varepsilon) , \quad (7)$$

where $v_H(r)=2\int v(r-r')n(r')dr'$ is the Hartree potential, i.e., the average Coulomb potential. In a crystal the Coulomb potential is the sum of the Hartree potential of electrons and the nuclear Coulomb repulsion

$$V_{nucl}=\tfrac{1}{2}\sum_{n,n'} Z_n Z_{n'} v(R_n,R_{n'}) ,$$

where R_n denotes the position of the nucleus n in the crystal lattice.

The simplest approximation for Σ is to neglect the second term in Eq. (7). The Hartree-Fock (HF) treatment consists of the assumption that

$$M^{HF}(r,r',\varepsilon)=i\delta(\varepsilon)v(r-r')G(r,r',\varepsilon) \equiv v_{ex}(r,r') \quad (8)$$

This simple approximation gives the HF exchange potential $v_{ex}(r,r')$ in Eq. (6). Note that the $v_{ex}(r,r')$ is nonlocal potential while the DFF exchange-correlation potential is local in principle.

In theories beyond the HF approach the self-energy should be regarded as a functional of Green function G. The functional can be written as a series expansion in a

$G(r,r',\varepsilon)$ and $v(r-r')$:

$$M(r,r',\varepsilon)=\sum_{n=1}^{\infty} M^{(n)}(G,v) \ . \tag{9}$$

Each term of the series expansion has a diagram representation, for example

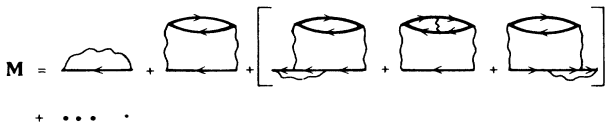

(10)

Here the terms with $n=1,2,3$ from expansion (9) are shown. The functions G are represented by the straight lines and the interaction $v(r,r')$ by the wavy curves.

It should be noted that the given expansion of M was made by expanding the dynamically screened interaction as a power series in $v(r,r')$.[23] In addition it should be also emphasized that the first term of the expansion (10) which gives the HF approximation (8), provides a reasonable description of a system. Thus, we obtain a complete set of the HF one-electron wave function $[\phi_k^{\rm HF}(r)]$ by solving the Schrödinger equation (6), and the Fourier transform of $v(r-r')$ is

$$v_k^{\rm HF}(q)=\int [\phi_k^{\rm HF}(r)]^* v(r-r')\phi_{k+q}^{\rm HF}(r')dr\,dr' \ . \tag{11}$$

Note that we have now the potential $v^{\rm HF}(q)$ which is not similar to free-electron potential $4\pi/q^2$ [$v_k^{\rm HF}(q)$ is less than the initial Coulomb potential]. Further, in this case the Hamiltonian, taking into account only the first term of (10), has the diagonal form on the basis of eigenfunctions $[\phi_k^{\rm HF}(r)]$ and a new set of quasiparticles and their interactions $v_k^{\rm HF}(q)$ are determined $[\varepsilon_k,\phi_k^{\rm HF}(r)]$. We may calculate now the second term of Eq. (10) with the Green functions of these states and the new interaction between them and we obtain again a new set of eigenfunctions and a new diagonal form of Hamiltonian. By using Eq. (10), it is possible to calculate the new interaction. The process may be continued for other terms of expansion (10).

If the effective crystal potential in Eq. (6) was constructed in the framework of DFF approach, we may obtain the complete and orthonormal set of eigenfunctions $[\phi_k^{\rm DFF}(r)]$ and determine some interaction function $v_k^{\rm DFF}(q)$ through Eq. (11). These functions can be used for calculations of diagrams in expansion (10), but now we do not know exactly what type of diagrams are included in our first approximation. Therefore the question is whether we have any possibility of constructing a perturbation series like in Eq. (10) for the one-particle band structure obtained in the framework of the DFF approach.

Ten years ago Yasuhara and Watabe[24] showed that the self-energy may be defined by the functional derivative

$$\frac{\delta E_{\rm xc}(G,v)}{\delta G(r,r',\varepsilon)}=-M(r,r',\varepsilon) \ , \tag{12}$$

where $E_{\rm xc}(G,v)$ is the functional of the exchange-correlation energy.

On the other hand, in the framework of DFF theory we have[3,9]

$$\frac{\delta E_{\rm xc}(G,v)}{\delta v(r,r')}=\frac{1}{2}n(r)n(r')[g(r,r')-1] \ . \tag{13}$$

Then we obtain the following expression:

$$i\int dr'\int d\varepsilon\, G(r,r',\varepsilon)\frac{\delta E_{\rm xc}(G,v)}{\delta G(r,r',\varepsilon)} =2\int dr''\, v(r,r'')\frac{\delta E_{\rm xc}(G,v)}{\delta v(r,r'')} \ . \tag{14}$$

From Eqs. (12)–(14) the self-energy can be expressed as

$$\tilde{M}(r,r',\varepsilon)=\delta(r-r')\delta(\varepsilon)\int dr''\, v(r,r'')n(r'')[g(r,r'')-1] \ . \tag{15}$$

The expression (15) is the same as the definition of exchange-correlation potential of DFF [Eq. (1)], i.e., $\tilde{M}(r,r',\varepsilon)\equiv v_{\rm xc}(r)$. It should be noted that (i) Eq. (15) is not the unique solution of Eq. (14); (ii) the self-energy of DFF theory $\tilde{M}(r,r',\varepsilon)$ contains all possible types of diagrams from expansion (9); (iii) from Eq. (15) it follows the existence of some conditions for the electron-electron interactions in the DFF approach.

At first the interaction must be local, i.e., the transmitted momentum $q=0$ or $r=r'$. In addition, the dynamic correlations are neglected, i.e., transmitted energy $\varepsilon=0$. It means that we can consider the diagrams with any index n and all types of corrections to the DFF band structure, if the electron-electron interaction characterizes the processes with $q\neq 0$ or $\varepsilon\neq 0$.

III. ELECTRONIC STRUCTURE

A. Linear-muffin-tin orbital (LMTO) calculation

In order to calculate the band structure we have used the self-consistent scalar-relativistic LMTO method with

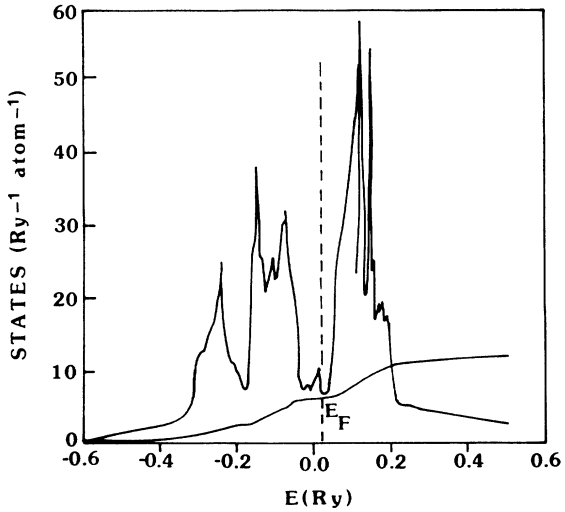

FIG. 1. Total density of states and number of electrons of commensurate antiferromagnetic chromium.

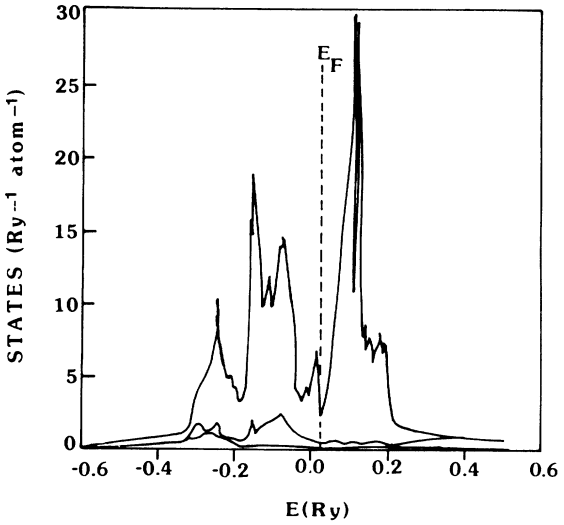

FIG. 2. Partial density of states of commensurate antiferromagnetic chromium.

combined corrections properly included.[24,25] The present calculation was made for the case of antiferromagnetic commensurate phase of chromium with the simple cubic CsCl lattice (experimental equilibrium radius $S=2.684$ a.u.). The one-electron technique is based on the local spin-density approximation to the DFF and the exchange-correlation derived by Von Barth and Hedin[26] was used.

We consider a frozen core and treat $4s$, $4p$, and $3d$ as band electrons. The self-consistency is attained with a small number of $\mathbf{k}$ points (i.e., 169) in the irreducible Brillouin zone (IBZ). The final bands are obtained after 15 iterations with a fine mesh of 969 $\mathbf{k}$ in the IBZ. The results of calculation are presented in Figs. 1 and 2 for the total and partial density of states and number of states and in Fig. 3 for the band schemes along some high-symmetry directions.

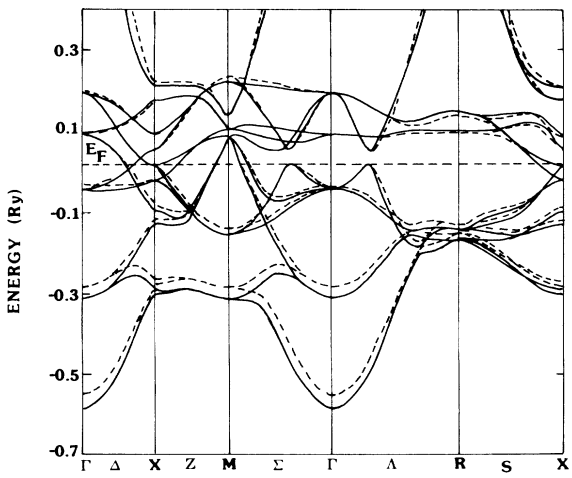

FIG. 3. The self-consistent energy bands in antiferromagnetic chromium along some high symmetry directions. Solid curve without self-energy corrections; dashed curve, with self-energy corrections.

B. Model for the calculation of many-particle corrections to the electronic structure

As was shown in Sec. II any type of diagram with $q\neq 0$ and/or $\varepsilon\neq 0$ is the correction to the LDA DFF band structure. Hedin and Lundqvist[23] have shown that corrections with $q\neq 0$ but $\varepsilon=0$ are relatively small.

Let us consider the Hamiltonian expressed in terms of annihilation and creation operators for the Bloch and/or Wannier states as

$$H=H_0+V\ , \tag{16}$$

where

$$H_0=\sum_{\sigma}\sum_{\mathbf{k},\nu}E_\nu(k)a^\dagger_{\nu\mathbf{k}\sigma}a_{\nu\mathbf{k}\sigma}=\sum_{\sigma}\sum_{j,l}\sum_{m,m'}t_{jl}^{mm'}a^\dagger_{jm\sigma}a_{lm'\sigma}\ , \tag{17}$$

and

$$V=\tfrac{1}{2}\sum_{\sigma,\sigma'}\sum_{j,l}\sum_{j',l'}\sum_{m,m'}\sum_{n,n'}V_{jll'j'}^{mnn'm'}a^\dagger_{jm\sigma}a^\dagger_{ln\sigma'}a_{l'n'\sigma'}a_{j'm'\sigma}\ , \tag{18}$$

$$V_{jl,l'j'}^{mn'm'}=2\int\int d\mathbf{r}\,d\mathbf{r}'\frac{1}{|\mathbf{r}-\mathbf{r}'|}W_m(\mathbf{r}-\mathbf{R}_j)W_n(\mathbf{r}'-\mathbf{R}_l)\times W_{n'}(\mathbf{r}'-\mathbf{R}_{l'})W_{m'}(\mathbf{r}-\mathbf{R}_{j'})\ . \tag{19}$$

The Bloch wave functions $u^\nu_{\mathbf{k}}(\mathbf{r})$ and Wannier $W_m(\mathbf{r}-\mathbf{R}_j)$ states are related by the following transformation:

$$u^\nu_{\mathbf{k}}(\mathbf{r})=\frac{1}{\sqrt{N}}\sum_{\mathbf{R}_j}W_\nu(\mathbf{r}-\mathbf{R}_j)e^{i\mathbf{k}\cdot\mathbf{R}_j}\ . \tag{20}$$

In order to utilize the Hubbard model for the Hamiltonian (16) to compute the many-particle corrections it should be shown that $v(\mathbf{r},\mathbf{r}')$ (see Sec. II) has an explicit connection with $V_{jll'j'}^{mnn'm'}$ matrix elements. According to our determination (11) $v(\mathbf{r},\mathbf{r}')$ is related with $v(\mathbf{q})$ as follows:

$$v_{\mathbf{k}}^{\nu\nu'}(\mathbf{q})=\int\int u^\nu_{\mathbf{k}}(\mathbf{r})\frac{1}{|\mathbf{r}-\mathbf{r}'|}[u^{\nu'}_{\mathbf{k}+\mathbf{q}}(\mathbf{r}')]^*d\mathbf{r}\,d\mathbf{r}'=\frac{1}{N}\int\int d\mathbf{r}\,d\mathbf{r}'\sum_{\mathbf{R}_j,\mathbf{R}_{j'}}e^{i\mathbf{k}\cdot\mathbf{R}_j}v_{jj'}^{\nu\nu'}(\mathbf{r},\mathbf{r}')e^{-i(\mathbf{k}+\mathbf{q})\mathbf{R}_{j'}}\ , \tag{21}$$

where

$$v_{jj'}^{\nu\nu'}(\mathbf{r},\mathbf{r}')=W_\nu(\mathbf{r}-\mathbf{R}_j)\frac{1}{|\mathbf{r}-\mathbf{r}'|}W_{\nu'}(\mathbf{r}'-\mathbf{R}_{j'}) \tag{22}$$

By using (22) for the interaction integrals (19) we obtain

$$V_{jll'j'}^{mnn'm'}=2\int\int d\mathbf{r}\,d\mathbf{r}'W_n(\mathbf{r}'-\mathbf{R}_l)\times v_{jl'}^{mn'}(\mathbf{r},\mathbf{r}')W_{m'}(\mathbf{r}-\mathbf{R}_{j'})\ . \tag{23}$$

Although the inter-atomic terms are not necessarily negligible, the useful simplification is to neglect them and to

take into account only the intra-atomic terms:

$$U_{mm'}=V_{jjjj}^{mm'm'm}=2\int\int d\mathbf{r}\,d\mathbf{r}'W_{m'}(\mathbf{r}'-\mathbf{R}_j)\times v_{jj}^{mm'}(\mathbf{r},\mathbf{r}')W_m(\mathbf{r}-\mathbf{R}_j)\ , \tag{24}$$

$$J_{mm'}=V_{jjjj}^{mm'mm'}=2\int\int d\mathbf{r}\,d\mathbf{r}'W_{m'}(\mathbf{r}-\mathbf{R}_j)\times v_{jj}^{mm}(\mathbf{r},\mathbf{r}')W_{m'}(\mathbf{r}-\mathbf{R}_j)\ .$$

It means that we neglect the q dependence of the corrections.

If we utilize the contact approximation for the interaction $v_{jj}^{mm'}(\mathbf{r},\mathbf{r}')=I_{jj}^{mm'}(\mathbf{r})\delta(\mathbf{r}-\mathbf{r}')$, we obtain

$$U_{mm'}=2\int dr\ W_{m'}(\mathbf{r}-\mathbf{R}_j)I_{jj}^{mm'}(\mathbf{r})W_m(\mathbf{r}-\mathbf{R}_j)\ . \tag{25}$$

A further simplification is to replace $U_{mm'}$ and $J_{mm'}$ by their averages U and J. In the following applications we will use only the $U_{mm'}$ interaction in the q representation.

Hence, according to Eq. (21) and using the contact approximation

$$v_{\mathbf{k}}^{\nu\nu'}(\mathbf{q})=\frac{1}{N}\sum_{\mathbf{R}_j}e^{-iq\mathbf{R}_j}\int d\mathbf{r}\,I^{mm'}(\mathbf{r})=\delta(\mathbf{q})U\ . \tag{26}$$

It should be noted that $I_{jj}^{mm'}=I^{mm'}$ for the periodic system; the interaction of Stoner is determined as $I=U/N$, i.e.,

$$v^{\nu\nu'}(\mathbf{q})=N\delta(\mathbf{q})\delta_{nn'}I\ . \tag{27}$$

It is obvious that the greatest contribution is given by the second diagram in expression (10). Let us calculate this correction, i.e.,

$$M^{(2)}(\mathbf{r}_1,\mathbf{r}_2,\omega)=G(\mathbf{r}_1,\mathbf{r}_2,\omega)\int\int d\mathbf{r}_3\,d\mathbf{r}_4\,d\omega'\,v(\mathbf{r}_1,\mathbf{r}_3)G(\mathbf{r}_3,\mathbf{r}_4,\omega)G(\mathbf{r}_4,\mathbf{r}_3,\omega-\omega')v(\mathbf{r}_4,\mathbf{r}_2) \tag{28}$$

or

$$M^{(2)}(q,\omega)=I\int\int d\mathbf{r}_1\,d\mathbf{r}_2\sum_{\mathbf{k},\mathbf{k}',\mathbf{k}''\mathbf{k}}u(r_1)u_{\mathbf{k}}^{*}(\mathbf{r}_2)e^{i\mathbf{q}\cdot\mathbf{r}_1}e^{-i\mathbf{q}\cdot\mathbf{r}_2}u_{\mathbf{k}'}(\mathbf{r}_1)u_{\mathbf{k}'}^{*}(\mathbf{r}_2)u_{\mathbf{k}''}(\mathbf{r}_2)u_{\mathbf{k}''}^{*}(\mathbf{r}_1)\frac{f_{k''}(1-f_{k'})(1-f_k)+(1-f_{k''})f_{k'}f_k}{\omega+E_{k''}-E_{k'}-E_k}\ . \tag{29}$$

In order to calculate the expression (29) we make the approximation

$$\pi=\int\int d\mathbf{r}_1d\mathbf{r}_2u_{\mathbf{k}'}(\mathbf{r}_1)e^{i\mathbf{q}\cdot\mathbf{r}_1}u_{\mathbf{k}''}^{*}(\mathbf{r}_1)u_{\mathbf{k}}^{*}(\mathbf{r}_2)e^{-i\mathbf{q}\cdot\mathbf{r}_2}u_{\mathbf{k}''}(\mathbf{r}_2)u_{\mathbf{k}'}(\mathbf{r}_1)u_{\mathbf{k}'}(\mathbf{r}_2)\leq|P(\mathbf{r}_1,\mathbf{r}_2,\mathbf{q})|^2\ , \tag{30}$$

where $P(r_1,r_2,q)$ is the dipole matrix element. This estimation seems to be more realistic than the standard assumption that all matrix elements are equal to 1. Thus, we obtain for any choice of bands with indexes i,j,k

$$M^{ijk}(\omega)=\frac{n_\sigma}{N_b}I^2\left[\int_{B_i}^{E_F}dE_1^i\int_{E_F}^{T_j}dE_2^j\int_{E_F}^{T_k}dE_3^k\,P^{ij}(\omega)\frac{N^i(E_1)N^j(E_2)N^k(E_3)}{\omega+E_1^i-E_2^j-E_3^k+i\delta}+\int_{E_F}^{T}dE_1^i\int_{B}^{E_F}dE_2^j\int_{B}^{E_F}dE_3^k\,P^{ij}(\omega)\frac{N^i(E_1)N^j(E_2)N^k(E_3)}{\omega+E_1^i-E_2^j-E_3^k+i\delta}\right]\ , \tag{31}$$

where $N^i(E)$ is the density of states of ith band, T and B are the top and bottom of the bands, $P^{ij}(\omega)$ is the energy dependence of the probability of transitions between ith and jth bands, i.e.,

$$P^{ij}(\omega)=\frac{\int d\mathbf{k}\,|P_{ij}(\mathbf{k})|^2\delta(E_k^i-E_k^j+\omega)}{\int d\mathbf{k}\delta(E_k^i-E_k^j+\omega)}\ . \tag{32}$$

The factors n_σ and N_b are the normalization factors, i.e., N_b is the number of bands taken into account and n_σ is the coefficient connected with spin degeneration of bands ($n_\sigma=2$ for intraband transitions and $n_\sigma=4$ for interband transitions).

It should be noted that a similar expression may be obtained in the framework of the one-band Hubbard model,[27] where all interband contributions are neglected; the case of degenerate d bands is considered and $P^{ij}(\omega)\equiv1$. Our numerical estimates show the significant influence of the interband processes. At the same time our calculations and results by Tréglia *et al.*[27] demonstrate that the simple local term (31) accounts for about 90% of the total value. The nonlocal terms create the q dependence of the corrections to self-energy, the dependence was neglected in our calculations.

In order to calculate $M^{ijk}(\omega)$ we assumed that $N^i(E)$ is the rectangular density of states (DOS) for a single band, and we introduced the abbreviations b_i,t_i to represent the bottom and the top of ith band. Further, h_i is the value of rectangular DOS normalized to one electron in band. The first term of $M^{ijk}(\omega)$, for example, can be written as

$$S_1(\omega)=\frac{n_\sigma I^2}{N_b}\sum_{i=1}^{N_2}h_j\sum_{k=N_1}^{N_b}h_k\int_a^b dz\int_c^d dy\int_f^g dx\frac{P^{ij}(\omega)}{\omega+z-y-x+i\delta}\ , \tag{33}$$

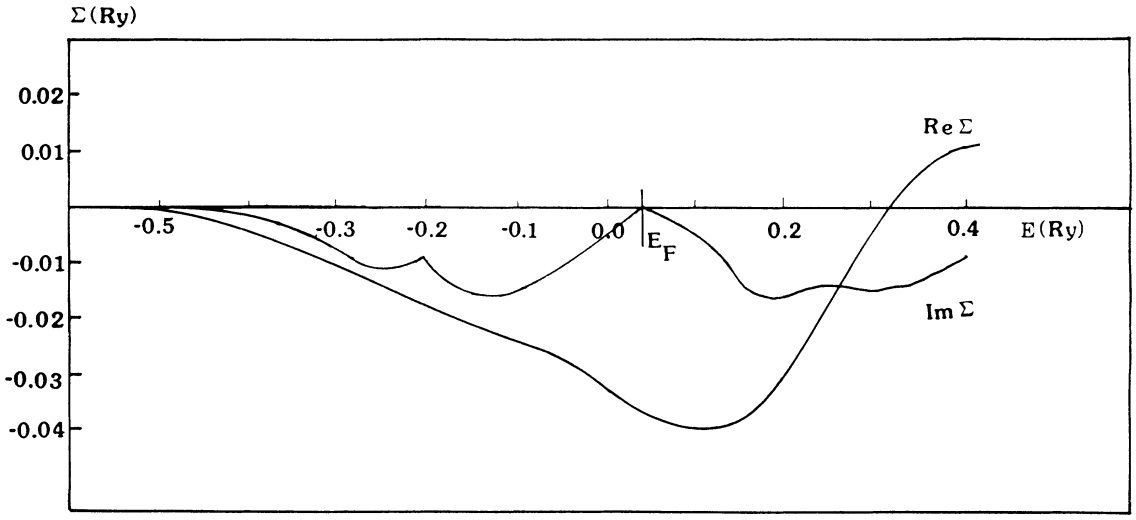

FIG. 4. Energy dependence of the self-energy of antiferromagnetic chromium.

where N_1 (and N_2) is the minimum (maximum) number of filled band and $a=b_i$, $b=t_i$ or E_F, $c=E_F$ or b_j, $d=t_j$, $f=E_F$ or b_k, $g=t_k$. It should be noted that the approximation of total density of states (DOS) as the sum of the rectangular partial DOS represents correctly the full model DOS and real DOS for the principal features (the peaks and so on).

One can see from Fig. 4 that the real and imaginary parts of self-energy have behavior which is expected to be in accord with general results.[11] Since the value of the Stoner parameter for the Coulomb potential is undetermined in our model, we have used an effective Stoner parameter of spin fluctuation determined self-consistently in our band-structure calculations.

C. Ground-state properties and band structure

We have collected some measured and calculated values of pressure P, sublattice magnetization M, effective Stoner interaction parameter I, and density of states at the Fermi level $N(E_F)$ for $S=2.684$ a.u. in the commensurate antiferromagnetic chromium in Table I. In this table we have also summarized the results of various calculations.[14,28,29] As can be seen, the agreement between present calculation and experiment is good. Our results are close to the results of Küber[29] which are obtained by using the LASW method and there are significant discrepancies between our calculation and an earlier LMTO calculation.[28] The reason of these discrepancies between the two LMTO calculations is not clear. However, it should be emphasized that in order to obtain full agreement between Skriver's calculation and experiment it is necessary to change the atomic radius S to within a few percent of the observed lattice space. Therefore the discrepancies may be explained by the accuracy in the numerical calculations.

On the other hand, the agreement between present theoretical results (and those of Kübler) and experimental values of density of states at the Fermi energy seems quite good. But it is strange because of the existence of the electron-phonon enhancement for the value of $N(E_F)$. In order to compare theory and experiment one must multi-

TABLE I. The ground-state properties of antiferromagnetic chromium for the experimental value of lattice constant ($a=2.884$ Å).

	Skriver[a]	Kübler[b]	Kulikov and Kulatov[c]	Present work	Experiment
P (kbar)	−147			−70	0
M (unit of μ_B)	0.29		0.48	0.593	0.59
I (mRy)	60.3	63.9	54.7	67.9	
$N(E)$ (states/Ry atom)	5.8	8.7	4	9.16	8.1[d]
					9.2[e]

[a]Reference 28.
[b]Reference 29.
[c]Reference 14.
[d]Reference 30.
[e]Reference 31.

TABLE II. l-projected number of states and density of states at the Fermi level.

		Skriver[a]		Present work	
	l_σ	$\sigma=\uparrow$	$\sigma=\downarrow$	$\sigma=\uparrow$	$\sigma=\downarrow$
n_l	s	0.31	0.31	0.315	0.309
(electron per	p	0.41	0.41	0.410	0.412
atom per spin)	d	2.42	2.13	2.571	1.982
$N_l(E)$	s	0.03	0.02	0.037	0.024
(states per Ry	p	0.47	0.46	0.418	0.518
per atom)	d	2.55	2.28	5.913	2.254

[a]Reference 28.

ply the theoretical $N(E_F)$ by $(1+\lambda)$, where λ is the coefficient of electron-phonon interaction which is close to 0.25 for the case of Cr.[32] The total density of states shown in Fig. 1 is similar to that obtained by Skriver,[28] Kübler,[29] and Kulikov and Kulatov.[14] It should be noted that the values $N(E_F)$ of LASW calculation[29] and present LMTO calculation are close to each other. We believe that the calculation of Kübler[29] is the most accurate since the results of band-structure calculation was used for the evaluation of the difference between the total energies of the antiferromagnetic and paramagnetic states. The result predicts the existence of antiferromagnetic ordering in the chromium.

Figure 2 contains the partial density of states. Some representative results obtained for the antiferromagnetic Cr are shown in Table II. It is obvious that there is considerable discrepancy between the absolute values of d-projected numbers of states and d density of states at the Fermi level (spin polarized) obtained by earlier LMTO calculation[28] and by the present authors. It is obvious also that the d states determine the total magnetization in antiferromagnetic sublattice. There is a peak of d type which appears in the antiferromagnetic case close to the Fermi level. This extra structure is caused by the energy gaps produced by exchange splitting of the paramagnetic band structure.

The band schemes of commensurate antiferromagnetic Cr obtained in the framework of LMTO method (solid curves) are presented in Fig. 3. In this figure we have also included the band structure corrected by the self-energy term (dashed curves). The degeneracies are lifted by the exchange interaction producing the gaps along Σ and Δ directions which stabilize the antiferromagnetic ordering. In Table III, we have summarized the results of various calculations including the ones presented here. It is helpful to compare these theoretical results with the experimental values[33–35] of the filled part of the d bands and also with the total filled-valence-band widths. The calculation in the framework of DFF approach gives the bandwidths longer than the experimental one (Table III).

When self-energy correction is taken into account the occupied bandwidth is sufficiently decreased and its value compares well with the experiment. Another interesting value is the filled part of the d bands. We obtain a better agreement with the experimental value. The calculated average value of the AF gap is equal to 0.45 eV and it is rather close to the theoretical ones by other authors and does not differ significantly from the experimental values for commensurate Cr-Mn alloys. The self-energy corrections do not change the value of the AF gap, since this effect is not very important near the Fermi surface.

IV. OPTICAL PROPERTIES

The optical density of states of antiferromagnetic chromium was calculated by interpolation over 969 **k** points in the irreducible part of Brillouin zone in the energy range from 0 to 0.5 Ry with an energy step of 0.0025 Ry, taking in all 12 bands between which there are transitions in this energy range.

TABLE III. Relative energies at Γ in AF Cr; Δ is the AF (antiferromagnetic) gap.

				Present work		
Energy (Ry)	Skriver[a]	Kübler[b]	Kulikov and Kulatov[c]	DFF[d]	SC[e]	Experiment
						0.50[f]
$E_F-E_{\Gamma_1}$	0.62	0.58	0.61	0.62	0.57	0.151[g]
$E_F-E_{\Gamma_{12}}$	0.33	0.31	0.35	0.33	0.31	0.331[h]
Δ	0.033	0.037	0.035	0.033	0.033	0.36[h]

[a]Reference 28.
[b]Reference 29.
[c]Reference 14.
[d]DFF is the density-function formalism.
[e]SC is the self-energy correction included.
[f]Reference 33.
[g]Reference 34.
[h]Reference 35.

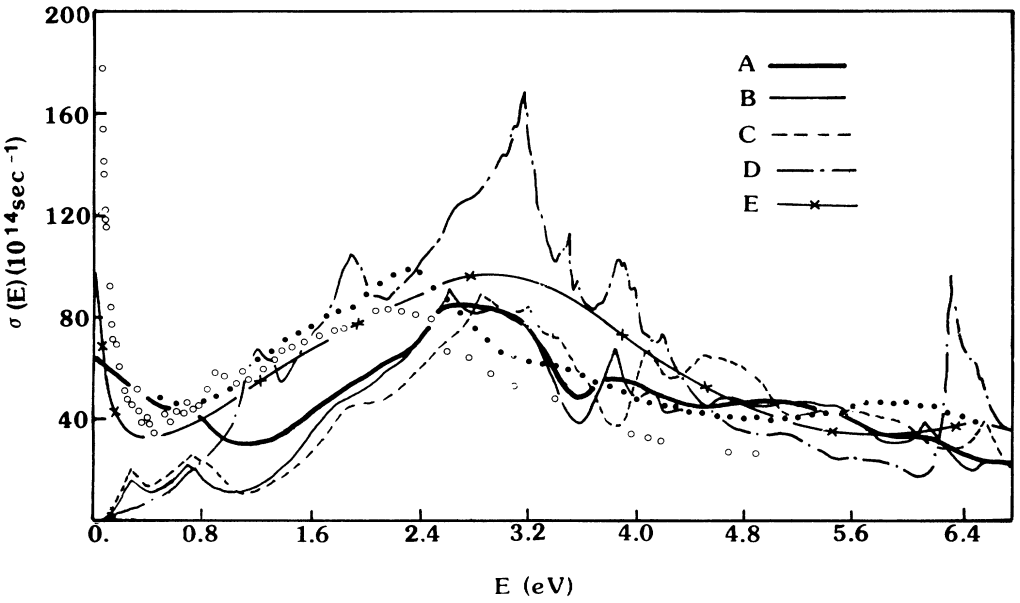

FIG. 5. The total interband optical conductivity $\sigma_1^0(\omega)$ with self-energy corrections (curve *A*), the interband part $\sigma_1^b(\omega)$ with (curve *B*) and without self-energy (curve *C*) corrections. Curve *D* shows $\sigma_1^b(\omega)$ as calculated by Laurent *et al.* (Ref. 16) and curve *E*, their total $\sigma_1(\omega)$. The experimental data of optical conductivity are as follows: Open circles, Ref. 18; solid circles, Ref. 37.

The interband part of the optical conductivity function $\sigma_1^b(\omega)$ in the limit of vanishing linewidth is

$$\sigma_1^b(\omega)=\frac{2\pi e^2}{3m^2\omega^2}\sum_{n,n'}\int_{\mathrm{BZ}}\frac{1}{(2\pi)^3}d\mathbf{k}\,|\,P_{nn'}(\mathbf{k})\,|^2 \times\delta(E_n(\mathbf{k})-E_{n'}(\mathbf{k})-\hbar\omega)\ , \tag{34}$$

where n and n' are occupied $[E_n(\mathbf{k})\leq E_F]$ and unoccupied $[E_{n'}(\mathbf{k})>E_F]$ energy bands, $E_n(\mathbf{k})$ represents the nth energy level at a given $\mathbf{k}$ vector and E_F is the Fermi level. ω is the photon frequency. $P_{nn'}(\mathbf{k})$ is the dipole matrix element which is obtained by using Wigner-Ekart theorem for the gradient formula.[36]

The function $\sigma_1(\omega)$ is depicted graphically in Fig. 5. Curves *B* and *C* are the interband conductivity obtained by using the Eq. (34), respectively, with and without self-energy correction. Curve *A* is the total conductivity including the intraband part (Drude term) and the effect of the lifetime broadening due to the electron-electron interactions. In Fig. 5 we have also presented the results of the calculations of the interband conductivity (curve *D*) and the total conductivity (curve *E*) of the paramagnetic chromium obtained by Laurent *et al.*[16] The available experimental data[18,37] (open circles and solid circles) are shown in the same figure.

As can be seen, the interband transitions occur just above the zero energy which means that there is no optical gap for the direct interband transitions. It should be noted also that we obtained the same structures of the optical conductivity function as Laurent *et al.*,[16] except in the region of low-energy transitions where we found some additional structures which characterize the antiferromagnetic chromium electronic bands. Note, that the experimental optical conductivity of the paramagnetic and antiferromagnetic chromium differs only at low energies of photons (i.e., $\omega\leq 0.5$ eV).[35,38]

The magnitude of the peaks of our curve (*C*) is smaller than that of curve *D*, but this result is in good agreement with the experimental measurements depicted in Fig. 5. In order to obtain a good agreement with experiments Laurent *et al.* introduced a fitting lifetime ($\tau^{-1}=0.5$ eV) which leads to the spreadoff of the initial curve and decreases the magnitude of the peaks as shown in Fig. 5.

Our principal peak at 3 eV in curve *C* is shifted towards higher energies about 0.7 eV from its experimental position but is in good agreement with the theoretical one of Laurent *et al.*[16] This peak can be associated with $T_5\rightarrow T_1$ transitions.

The peak at 4 eV is also shifted towards the higher energies from the experimental one at 3.5 eV and it is possible to associate this peak with same type of transitions ($T_5\rightarrow T_1$) as the principal peak at 3 eV. The high energy experimental structure at 6 eV is described by the interband transitions $Z_1\rightarrow Z_3$ and $Z_3\rightarrow Z_{1'}$ and it is displaced in the theoretical calculations on the higher energies by 0.5 eV.

In the region of low energies we obtained two peaks at 0.40 and 0.8 eV. The structure of 0.8 eV exists in both paramagnetic and antiferromagnetic measurements at 1 eV;[35,38] Laurent *et al.* obtained this peak at 1.2 eV in their paramagnetic chromium calculations. The lowest-energy peak is typically antiferromagnetic, because it is connected with the appearance of the antiferromagnetic gap at the Fermi energy as discussed in the previous section (see also Fig. 3). The position of this peak is in an

excellent agreement with the structure which was found in the optical measurements of the commensurate phase of Cr stabilized by impurities.[35,38]

The predicted positions of peaks deviate more from the experiments when the excitation energy becomes larger (it means that the principal errors connected with DFF approach exist). Let us utilize the self-energy corrections which were obtained in the preceding section. In order to take into account the many-particle effects for the calculation of the optical conductivity we changed the values of energies $E_n(\mathbf{k})$ by using the following procedure:

$$\tilde{E}_n(\mathbf{k}) = E_n(\mathbf{k}) + \mathrm{Re}\,|\,M^{(2)}(E)\,|\ , \tag{35}$$

and we utilized the new values $\tilde{E}_n(k)$ in expression (34). We neglected the k dependence of the self-energy correction. The results of this calculation are presented in Fig. 5 (curve *B*).

It should be noted that the agreement between theoretical and experimental structures is improved: There is the shift of the theoretical peaks to lower energies, and therefore the predicted peaks are closer to the experimental ones. However, these shifts must be larger for a better agreement between calculations and measurements.

Curve *A* represents the final result of our calculation in which the lifetime effect, i.e., the value of $1/\tau = \langle\,\mathrm{Im}\,|\,M^{(2)}(E)\,|\,\rangle$, has been taken into account together with the Drude intraband contribution. The free-electron relaxation time was given by Lenham and Treherne.[39] The shift of energy spectrum has the correct tendency, but it is only half of what it should be to give a perfect agreement with the experimental data.

V. CONCLUSION

There is no doubt that it is possible to get a good agreement between the theory and experiment using the parameters I and $1/\tau$ as the fitting parameters. Such an approach for the ferromagnetic Fe, Co, and Ni was recently used by Tréglia *et al.*[40] on the basis of degenerated Hubbard model and LDA DFF band structures, but the goal of this work is different. In this work we are interested in the *ab initio* values of many-particle corrections to improve the one-particle DFF band structure.

In the present study it is shown that some many-particle effects are not taken into account by DFF theory in principle. Simultaneously there is the error introduced in the calculation by the LDA approach in the framework of DFF theory. It is possible that we can obtain the good quantitative agreement between DFF theory and experiments for the electronic properties beyond the LDA approach,[19,20] but the influence of many-particle corrections depends critically on the value of interaction constant I, and in the case of ferromagnetic or antiferromagnetic metals its value may be large as it is demonstrated here.

ACKNOWLEDGMENTS

The authors are very thankful to Professor N. H. March for a critical reading of the manuscript. Two of us (M.A. and M.A.K.) benefited from a short stay at the International Centre for Theoretical Physics (ICTP) (Trieste). The Laboratoire de Magnetisme et de Structure Electronique des Solides is "unité associé au Centre National de la Recherche Scientifique No. 306."

*Permanent address: L. F. Veregschagin Institute of High Pressure Physics, Academy of Science of USSR, 142092 Troitsk, Moscow Region, USSR.

[1]P. Hohenberg and W. Kohn, Phys. Rev. **136**, 8864 (1964).
[2]W. Kohn and L. J. Sham, Phys. Rev. **140**, 1133 (1965).
[3]J. Callaway and N. H. March, Solid State Phys. **38**, 136 (1984).
[4]N. I. Kulikov, Izv. Vyssh. Uchebn. Zaved. Fiz. **12**, 50 (1982); [Sov. Phys. J. **25**, 1112 (1982)].
[5]C. S. Wang and P. E. Picket, Phys. Rev. Lett. **51**, 597 (1983).
[6]C. Svinati, H. J. Mattausch, and M. Hanke Solid State Commun. **51**, 23 (1984).
[7]M. S. Hybertsen and S. G. Louie, Phys. Rev. Lett. **55**, 1418 (1985).
[8]M. S. Hybertsen and S. G. Louie, Phys. Rev. B **34**, 5390 (1986).
[9]O. Gunnarsson and B. I. Lundqvist, Phys. Rev. B **10**, 4274 (1976).
[10]A. J. Mc Alister, J. R. Cuthill, R. C. Dobbyn, and M. W. Williams, Phys. Rev. B **12**, 2973 (1975).
[11]V. L. Moruzzi, J. F. Janak, and A. R. Williams, *Calculated Electronic Properties of Metals* (Pergamon, New York, 1978).
[12]D. Bagayoko, D. G. Laurent, S. P. Singhal, and J. Callaway, Phys. Lett. **76A**, 187 (1980).
[13]N. I. Kulikov and E. T. Kulatov, J. Phys. F **12**, 2267 (1982).
[14]N. I. Kulikov and E. T. Kulatov, J. Phys. F **12**, 2291 (1982).
[15]C. S. Wang and J. Callaway, Phys. Rev. B **15**, 298 (1977).
[16]D. G. Laurent, J. Callaway, J. L. Fry, and N. E. Brener, Phys. Rev. B **23**, 4977 (1981).
[17]A. Yu Uspenski, E. G. Maksimov, S. N. Rashkeev, and I. I. Mazin, Z. Phys. B **53**, 263 (1983).
[18]G. V. Gonin, M. M. Kirillova, L. V. Nomerovannaya, and V. P. Shirokovskiy, Fiz. Met. Metalloved. **43**, 907 (1977) [Phys. Met. Mettallogr. (USSR) **43**, 4 (1977)].
[19]G. Borstel, M. Newman, and W. Brawn, Phys. Rev. B **23**, 3113 (1981).
[20]G. P. Kerker, Phys. Rev. B **24**, 3468 (1981).
[21]R. Lässer, N. V. Smith, and R. L. Benbow, Phys. Rev. B **24**, 1895 (1981).
[22]N. V. Smith, R. Lässer, and S. Chiang, Phys. Rev. B **25**, 793 (1982).
[23]L. Hedin and S. Lunqvist, Solid State Phys. **23**, 2 (1969).
[24]O. K. Andersen, Phys. Rev. B **12**, 3060 (1975). O. K. Andersen and O. Jepsen, Physica **91B**, 317 (1977).
[25]H. L. Skriver, *The LMTO Method* (Springer-Verlag, Berlin, 1984).
[26]U. Von Barth and L. Hedin, J. Phys. C **5**, 1629 (1975).
[27]G. Tréglia, F. Ducastelle, and D. Spanjaard, J. Phys. (Paris) **41**, 281 (1980).
[28]H. L. Skriver, J. Phys. F **11**, 97 (1981).
[29]H. Kübler, J. Magn. Magn. Mater. **20**, 277 (1980).
[30]F. Heiniger, E. Bucher, and J. Muller, Phys. Lett. **19**, 163 (1965).
[31]J. K. Hulm and K. D. Blangher, Phys. Rev. **123**, 1539 (1961).
[32]W. L. Mc Millan, Phys. Rev. **167**, 331 (1968).
[33]C. Bonnelle and C. Hague, *Electronic Structure of Transition*

Metals, Its Alloys and Compounds (Naukova, Kiev, 1974), pp. 78.
[34]D. W. Fisher, Phys. Rev. B **4**, 1778 (1971).
[35]L. W. Bos and D. W. Fynch, Phys. Rev. B **2**, 4567 (1970).
[36]C. Koenig and M. A. Khan, Phys. Rev. B **27**, 6129 (1983).
[37]J. E. Nestell, Jr. and R. W. Christy, Phys. Rev. B **21**, 3173 (1980).
[38]L. V. Nomerovannaya, M. M. Kirillova, and T. A. Kozhevnikova, Fiz. Met. Metalloved. **42**, 732 (1976) [Phys. Met. Mettalogr. (USSR) **42**, 48 (1976)].
[39]A. P. Lenham and D. M. Treherne, in *Optical Properties and Electronic Structure of Metals and Alloys,* edited by F. Abélès (North-Holland, Amsterdam, 1966).
[40]G. Tréglia, F. Ducastelle, and D. Spanjaard, J. Phys. (Paris) **43**, 341 (1982).